

# Study on a novel exterior RCS hybrid joint by ABAQUS

Nguyen Viet Phuong

## Abstract

Hybrid RCS frames consisting of reinforced concrete (RC) column and steel (S) beam are used frequently in practice for mid- to high-rise buildings because of their several advantages. One of the key elements in RCS frames is the beam-column joints. This paper provides the validation of ABAQUS 3D finite element model by the experimental results.

Test specimens consist of four specimens of new exterior RCS hybrid joint that the European Project SMARTCOCO investigated with the aim to ease the construction process and avoid additional on-site work. A steel profile is welded to the steel beam and totally encased into a RC column. Four full scale exterior hybrid joints were tested at Structures Laboratory of the INSA de Rennes under monotonic loading. Finally some parametric studies were conducted to find out the suitable configuration of the steel part and the effects of concrete class to the joint behavior.

**Key words:** Exterior RCS hybrid joint, ABAQUS software, 3D finite element,  $L_e$  length

## 1. Introduction

Hybrid RCS frames consisting of reinforced concrete (RC) column and steel (S) beam are used frequently in practice because of their advantages such as reduction in structure's weight, covering large spans, increasing the lateral stiffness, convenience in adoption of strong column- weak beam criterion in tall buildings and enhanced ductility and energy dissipation capacities[1]. One of the key elements in RCS frames is the beam-column joints. The connections between a RC column and a steel beam can be classified into two types: continuous beam through (CBT) and continuous column through (CCT). In CBT connections, the beam runs through the joint continuously and the column envelopes the beam at the connection. It provides a ductile behaviour under seismic loading but orthogonal moment connection in the panel zone may be labor-intensive. The CBT joints are primarily problematic due to possible congestion of vertical rebars passing through the continuous beam and difficulties in pouring and compacting concrete in such location, especially for the middle CBT connection[1]. On the contrary, with the CCT connection, the column runs continuously through the joint. The face bearing plates (FBP), cover plate or shear studs are placed in the joint area. The beams are connected directly to the plates by penetration weld.

A number of joint configurations have been presented in many articles of many researchers such as Kanno and Deierlein (2000), Nishiyama et al (2004), Mirghaderi and Eghbali (2013), Zibasokhan et al (2016) and their respective advantages, shortcomings listed. Nearly all proposed solutions require significant additional on-site labor work. The European Project SMARTCOCO (2012-2016) investigated the behavior of a new RCS joint belonging to the CBT group of joints with the aim to ease the construction process and avoid additional on-site work. In this type of joint, a steel profile named by the embedded steel profile is welded to the beam and totally encased into the RC column (see Figure 1). Some shear studs along the embedded steel profile are also used to improve the strength and the ductility of the joint.

This paper provides the comparison between the numerical results using ABAQUS and the experimental results from four specimens of new exterior RCS hybrid joint. Four full scale exterior hybrid joints were prepared and tested at Structures Laboratory of the INSA de Rennes. After that, some parametric studies were conducted to find out the configuration of the steel part that leads to the better performance of the beam-column joint and the effects of concrete class to the joint behavior.

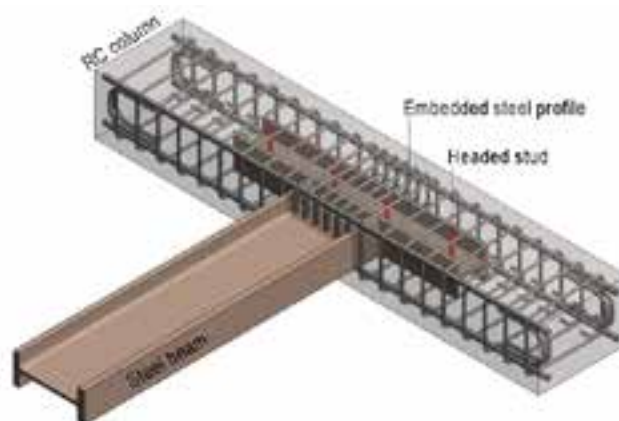


Figure 1. Novel exterior RCS joint detail proposed within SMARTCOCO project

Lecturer, faculty of civil engineering,  
Hanoi Architectural University,  
Email: [nguyenphuong.bt.hau@gmail.com](mailto:nguyenphuong.bt.hau@gmail.com)  
ĐT: 0914859909

Date of receipt: 16/4/2021  
Editing date: 20/5/2021  
Post approval date: 5/9/2022

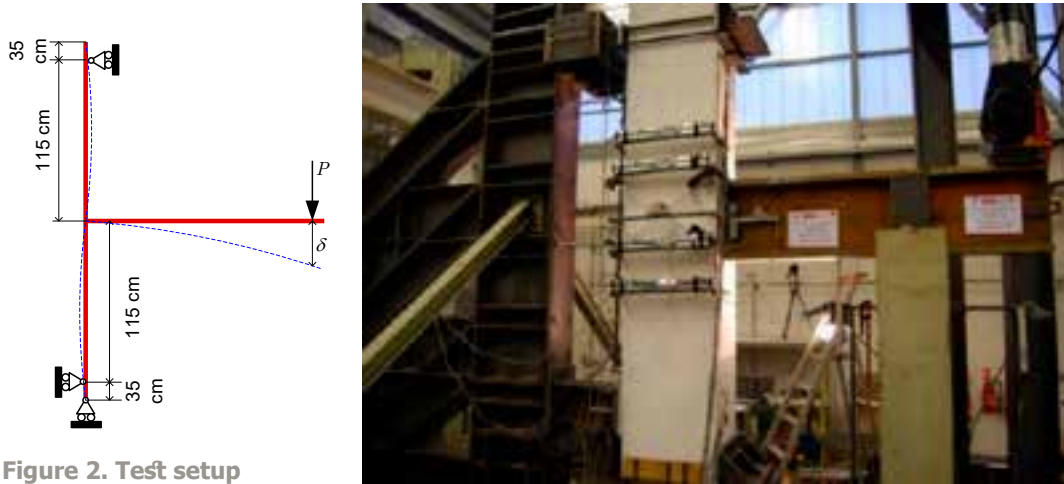


Figure 2. Test setup

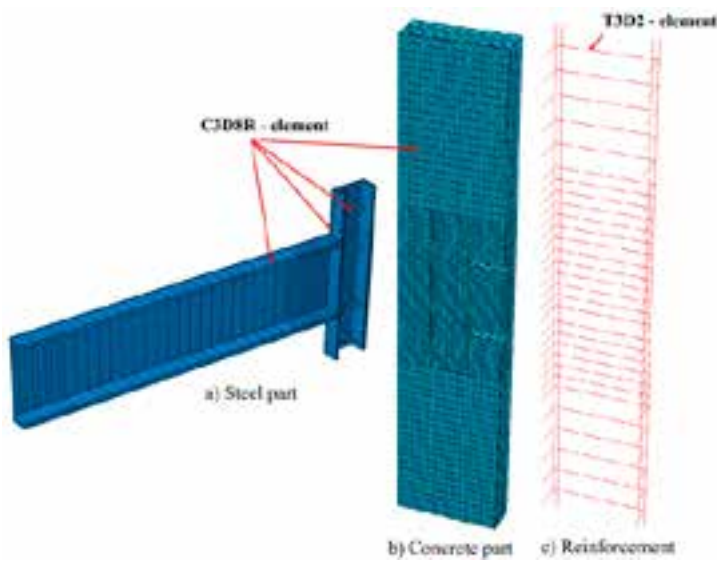


Figure 3. Finite element type and mesh of all components

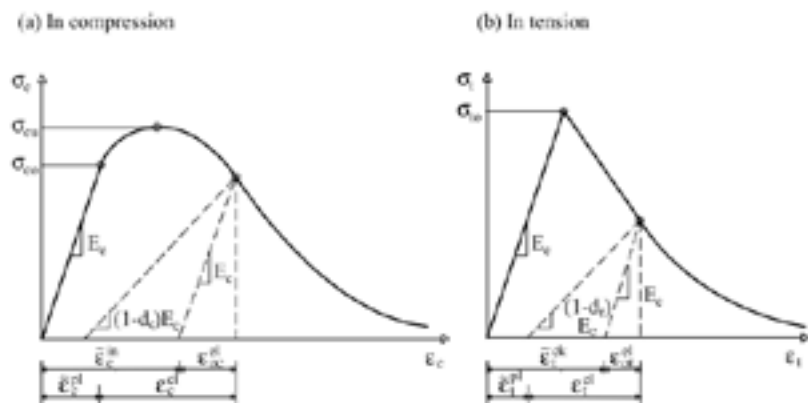


Figure 4. Stress-strain curve of concrete under uniaxial loading [8]

## 2. Experimental test of novel RCS hybrid joint

Four exterior RCS hybrid joints between steel beam and reinforced concrete column were tested at the Structures Laboratory of INSA Rennes from the end of 2015 to the beginning of 2016. The specimens are planar beam-column connections with 40cm x 60cm rectangular column with 3m length and HEM450 steel beam with 2m length (modified to

200mm flange width). All specimens have the same size, geometry and longitudinal reinforcing bar arrangements. The primary differences between the specimens are the concrete resistance (C40 and C60) and the total length (anchorage length) of the embedded profile in the RC column ( $L_e = 1\text{m}$  and  $1,5\text{m}$ ). The embedded steel profile is HEM200. The four specimens are labelled: HJS1 (with  $L_e=1\text{m}$  and C40), HJS2 (with  $L_e = 1\text{m}$  and C60), HJS3 (with  $L_e=1,5\text{m}$  and C40) and HJS4 (with  $L_e=1,5\text{m}$  and C60).

For all specimens, eight  $\phi 32$  bars were used for the longitudinal reinforcement. The shear reinforcements consist of  $\phi 16$  provided at 70mm spacing inside the joint region and at 140mm spacing in the reinforced concrete part outside the joint region. At both ends of the column,  $\phi 20$  U-bars were used for anchorage. Steel grade S460 and S500B were used for steel profiles and reinforcing bars, respectively. Several different instruments were used in the testing of the specimens. They can be divided into 4 types: (1) six inclinometers for recording absolute rotation at six cross-sections; (2) thirteen displacement sensors LVDTs (three for controlling the beam displacement, two for measuring the joint distortion and eight for determining the concrete column's displacement); (3) seventeen single strain gages for monitoring the transverse and longitudinal stresses; (4) five rosette gages for measuring the shear stresses. Monotonic concentrated load was put on the end of the steel beam by a hydraulic of 1500 capacity. The loading was applied in displacement-controlled manner by 3 steps: Firstly, did two initial cycles with an amplitude 1mm and displacement speed of 0,05mm/s; secondly, did the monotonic loading up to a displacement of 60mm with a speed of 0,02mm/s and finally, did the monotonic loading up to a displacement of 60mm up to 200mm with a speed of 0,1mm/s. The test setup was shown in Figure 2.

### 3. Finite element model for RCS hybrid joint by ABAQUS

ABAQUS is a powerful numerical tool used for component and system modeling and finds application in various fields. It is used to solve multi-degree and multi-physics transient problems. ABAQUS has several built-in models to predict the behavior of materials as well as the provision to add user defined models. The program offers a wide range of options regarding element types, material behavior and numerical solution controls, as well as graphic user interfaces, auto-meshers, and sophisticated post-processors and graphics to speed the analyses[2]. In this article, this commercial software is employed to develop reliable three-dimensional finite element model for the hybrid steel-concrete specimens of the experimental program.

#### a) Selection of finite element type and meshing

Because of the symmetry of the specimen geometry, support conditions and loading, only half specimen is modelled with the purpose of saving the computing. Each component of specimens consisted of concrete column, reinforcing rebars, steel beam, embedded steel profile and headed studs are modelled separately and assembled to produce the complete specimen model. The reinforced concrete column, the steel beam, the embedded steel profile were modelled by solid C3D8R element and T3D2 elements were chosen for the reinforcing bars (shown in Figure 3). In order to achieve the reliable results, the fine mesh was created in the connection zone. The mesh size depends on each element, each different increment and is from about 5mm to about 50mm.

#### b) Material modeling

In finite element model, concrete needs to be modelled with the Concrete Damaged Plasticity (CDP) parameters. The value of these parameters found out in articles of [3], [4], [5], [6] and [7] can be shown in Table 1. The uniaxial stress-strain curve of concrete in compressive and tensile behavior with two uniaxial damage variables in tension and

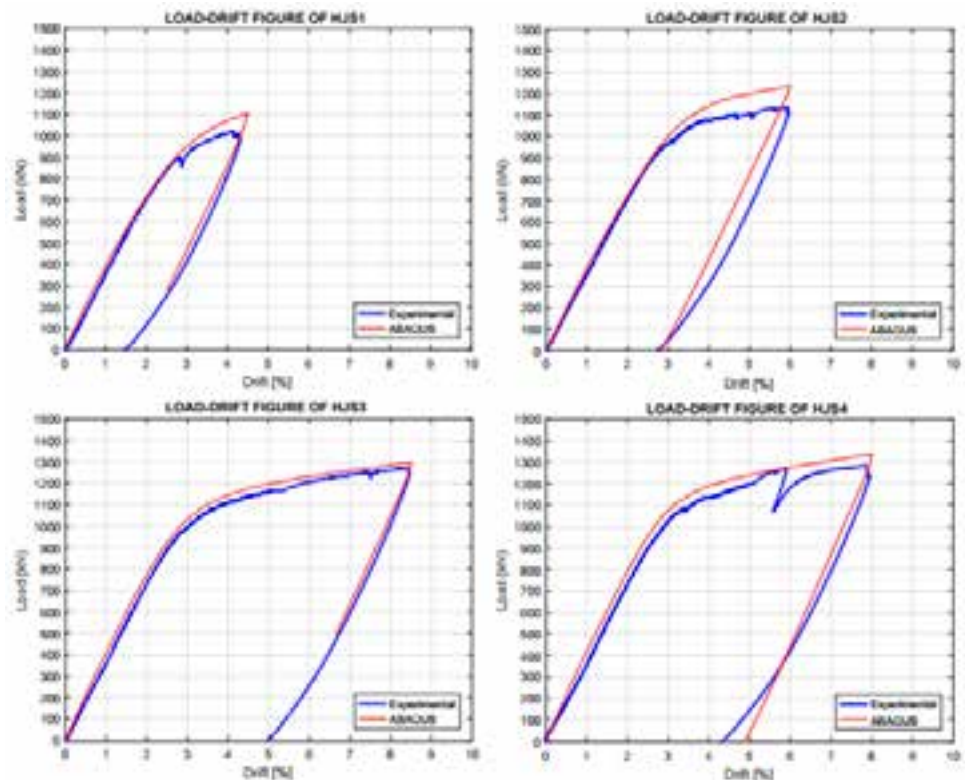


Figure 5. Numerical-experimental comparison of load-drift curve

compression can be determined by Eurocode 2 [8] and by Kratzig and Polling (2004) [9] (shown in Figure 4). These two uniaxial damage variables in compression and tension are specified in the options "Concrete Compression Damage" and "Concrete Tension Damage" in ABAQUS. The Poisson's ratio of concrete is taken equal to 0.2.

Table 1. The Concrete Damaged Plasticity in ABAQUS

| Dilation angle | Eccentricity | $f_{b0} / f_{c0}$ | K      | Viscosity parameter |
|----------------|--------------|-------------------|--------|---------------------|
| 36             | 0.1          | 1.15              | 0.6667 | 0.01                |

The Von-Mises yield criterion with isotropic hardening rule is used for modeling the structural steel included steel beam and encased steel profile, the reinforcement and the headed studs connected to the steel profile. In ABAQUS, the yielding stress and the elastic modulus are taken equal to 460 MPa and 210000 MPa for structural steel, respectively. For the reinforcing steel bar and headed studs, these parameters are taken equal to 500 MPa for the yield stress and 200000 MPa for the Young Modulus. For simplicity, the elastic-perfectly plastic model is used for the reinforcements and the elastoplastic model with hardening is considered for the structural steels.

Table 2. Numerical-experimental comparison of the initial stiffness and the applied loads at 4% drift

| Specimen | Applied load at 4% drift |                |           | Initial stiffness      |                     |           |
|----------|--------------------------|----------------|-----------|------------------------|---------------------|-----------|
|          | Experimental (kN)        | Numerical (kN) | Error (%) | Experimental (kNm/rad) | Numerical (kNm/rad) | Error (%) |
| HJS1     | 1011.04                  | 1070.52        | 5.88      | 213.91                 | 221.89              | 3.73      |
| HJS2     | 1076.16                  | 1146.19        | 6.51      | 215.98                 | 226.41              | 4.83      |
| HJS3     | 1114.43                  | 1149.92        | 3.18      | 303.03                 | 311.26              | 2.72      |
| HJS4     | 1135.56                  | 1189.42        | 4.74      | 345.42                 | 349.21              | 1.10      |

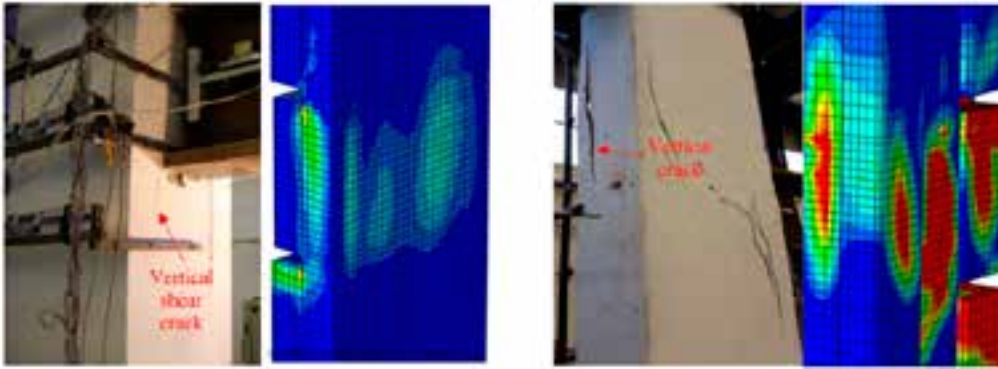


Figure 6. Comparison between crack pattern and damage plastic zone in ABAQUS

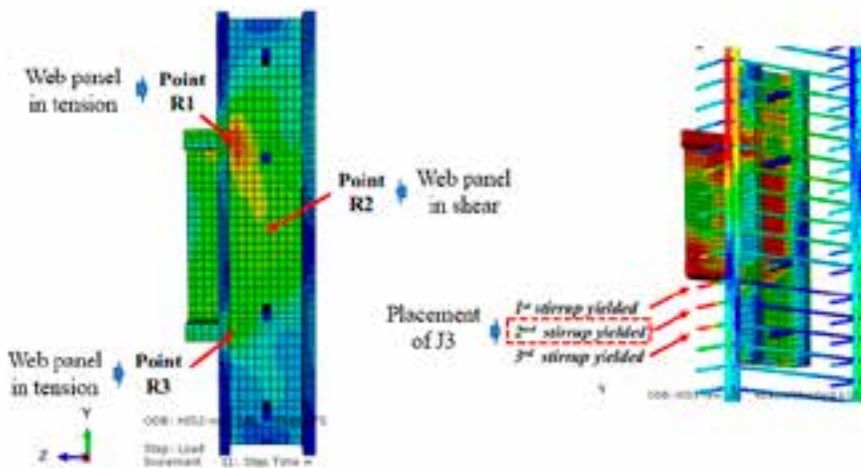


Figure 7. Location of the rosettes R1, R2, R3 and the strain gage J3

*c) Interaction conditions between components, boundary conditions and loading*

In addition, contact interactions between components play an important role in the specimen behavior, especially for the composite models. In this study, the reinforcing bars such as vertical longitudinal bars and stirrups are fully anchored in concrete so that embedded constraint method can be used for the interaction between rebars and concrete surrounding. For the interaction between concrete column, encased steel profile and shear studs, the general-self contact elements (available in ABAQUS library) are chosen to model the interaction between these components. The extremities of column is restrained in both vertical and horizontal directions by means of hinges. As mentioned before, symmetric of the specimen is exploited and only half of specimen can be modelled. Instead of applying a force at the steel beam end, a vertical displacement is applied to each node of the end cross-section of the steel beam.

**4. Validation of the numerical results by experimental test**

In order to validate the accuracy of the finite element model, four test specimens weremodelled. The results obtained in the numerical analysis, in terms of load-drift responses ofthe stresses at several points, were compared with the results obtained in the experimentaltests in the same terms. As can be seen in Figure 5 and Table 2, the numerical results were in good agreement with the experimental ones, both in terms of initial stiffness and ultimate loads. The initial stiffness can be defined as the intersection point between

the initial tangent at the beginning of the joint moment-joint rotation curve with the slope of  $k_j$  and the tangent in the inelastic domain presented by the slope of  $k_{j=10}$ . It can be noticed that the initial stiffness obtained in the numerical analysis is higher than the one obtained in the experimental tests. This difference appears due to the fixing set between the test specimen and the supports. If the results obtained in the numerical analysis and in the experimental tests are compared at the limit stage, it can be observed that the values of the ultimate forces and ultimate displacements are quite close for all tested elements.

Four main types of cracks were observed from the experimental tests: (1) horizontal cracks under the beam flange; (2) diagonal shear cracks in the shear panel; (3) vertical cracks below the steel beam bottom flange; and (4) splitting cracks due to loss of adhesion between reinforcement and concrete. Figure 6 shows three types of cracks (first, third and fourth ones) observed from the experimental test and damage plastic zones observed from the numerical model by ABAQUS. The location of cracks and damage plastic zones and also the value of applied load corresponding to their appearance time are quite similar in all specimens. In addition, in order to compare the behavior of the encased steel profile and stirrups with the experimental results, we look at the Von Mises stress evolution of the three points where the rosettes R1, R2 and R3 were pasted and the point of the strain gage J3 (shown in Figure 7).

Table 3 presents the numerical-experimental comparison of the applied loads leading to different yielding and the drifts corresponding to different component strength: steel web panel in tension; steel web panel in shear; steel web panel in compression; and second yielded stirrup. The error between experimental and numerical is from 0.68% to 12,12%. The sequence of yielding appearance in steel profile is also similar for all specimens. Good agreement between the numerical study and experimental test can be observed.

Due to all previous comparison results between experimental and numerical study, they mean that the numerical analysis by ABAQUS can be a reliable method to predict the exterior RCS hybrid joint behavior.

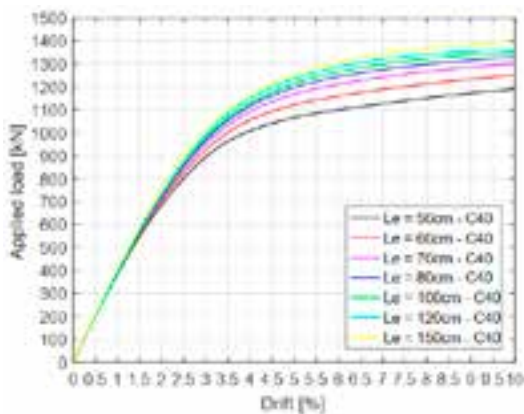


Figure 8. Load-drift curves for different anchorage length



Figure 9. Plastic bending moment and initial stiffness in cases of different anchorage length

### 5. Parametric studies for novel RCS hybrid joint

Using the 3D FE model which was successfully validated against experimental results of the studied RCS joint, a set of parametric studies was undertaken to understand the behavior of the joint as the components of the joint varied. The goal of this parametric study is to find out the configuration of the steel part that leads to the better performance of the beam-column joint. Therefore, the geometrical properties of the beam and the RC column are unchanged. The behavior of the joint is firstly investigated for the change of the length of encased profile. Because the height of steel beam is 478mm, the first value of encased steel profile's length is chosen from 500mm to the maximum of 1500mm. Let consider the

parametric study in case of the concrete class of C40 with the different anchorage length. Then, the influence of the concrete class on the joint response is studied. In addition to the case of 1m and 1,5m anchorage length which are presented above, five other cases are considered:  $Le = 0,5m$ ,  $Le = 0,6m$ ,  $Le = 0,7m$ ,  $Le = 0,8m$  and  $Le = 1,2m$ . Corresponding to each case of anchorage length, four concrete class are considered: C30, C40, C50 and C60. The input values of material have been taken from the Eurocode standard.

As can be seen in Figure 8 and Figure 9, the global behavior keeps almost unchanged when  $Le$  is greater than 80cm. In the opposite side, the different behavior between the cases of the anchorage length that is less than 80cm

Table 3 - Numerical-experimental comparison of the yielding time

|                                 | Specimen | Applied load      |                |           | Drift             |                |           |
|---------------------------------|----------|-------------------|----------------|-----------|-------------------|----------------|-----------|
|                                 |          | Experimental (kN) | Numerical (kN) | Error (%) | Experimental (kN) | Numerical (kN) | Error (%) |
| Column web panel in tension     | HJS1     | 633.4             | 574.3          | -9.33     | 1.79              | 1.54           | -14.0     |
|                                 | HJS2     | 645.3             | 652.7          | 1.15      | 1.81              | 1.78           | -1.66     |
|                                 | HJS3     | 668.8             | 639.3          | -4.41     | 1.88              | 1.61           | -14.4     |
|                                 | HJS4     | 683.7             | 696.5          | 1.87      | 1.87              | 1.74           | -6.95     |
| Column web panel in shear       | HJS1     | 844.9             | 830.8          | -1.67     | 2.53              | 2.43           | -3.95     |
|                                 | HJS2     | 878.7             | 945.0          | 7.55      | 2.55              | 2.76           | 8.24      |
|                                 | HJS3     | 871.4             | 893.2          | 2.50      | 2.51              | 2.39           | -4.78     |
|                                 | HJS4     | 835.7             | 937.0          | 12.12     | 2.31              | 2.44           | 5.63      |
| Column web panel in compression | HJS1     | 825.6             | 805.8          | -2.40     | 2.45              | 2.33           | -4.90     |
|                                 | HJS2     | 969.3             | 962.7          | -0.68     | 3.10              | 2.83           | -8.71     |
|                                 | HJS3     | 889.4             | 924.1          | 3.90      | 2.44              | 2.50           | 2.46      |
|                                 | HJS4     | 960.0             | 991.0          | 3.23      | 3.13              | 2.62           | -16.3     |
| Yielding of J3                  | HJS1     | 1017              | 1040.0         | 4.32      | 3.68              | 3.91           | 6.25      |
|                                 | HJS2     | 1118              | 1218.0         | 9.44      | 5.54              | 4.11           | -25.8     |
|                                 | HJS3     | 1131              | 1173.2         | 3.73      | 4.84              | 5.45           | 12.6      |
|                                 | HJS4     | 1251              | 1272.3         | 1.70      | 6.06              | 6.89           | 13.7      |

can be observed. It can be explained that the encased steel profile can be considered to be totally anchored into the RC column in cases of length more than 80cm. Therefore, the behavior of the hybrid joint can be considered similarly to the composite joint. Furthermore, it is observed that the stiffness of the joint is not much influenced by the anchorage length.

For the encased steel profile, the similar first yielding point can be found at the location of the point R1 in all specimens. It is noted that the yield stress at the point R1 corresponds to the yielding of the steel web panel in tension and this observation is also found in the experimental test. After that, the point R2 (web panel in shear) and R3 (web panel in compression) are the next ones reached to the yield stress. Figure 10 shows the bending moment corresponding to the yield stress at the locations of three point R1, R2, R3 and two first yielding stirrups in cases of different anchorage length. The quite similar behavior for the bending moment and the sequence of yielding appearance can be collected with the differences of anchorage length. The resistance of steel web panel almost increases followed by the increase of anchorage length of encased steel profile. For the stirrup stresses, two stirrups below the steel beam bottom flange yielded first because of the high compressive pressure caused by the rotation of the steel beam. As can be seen, the stress of the stirrups below the steel beam depends on the anchorage length of the encased steel profile.

As can be seen in Figure 11, the global behavior of the joint is much influenced by the concrete class in case of the anchorage length which is less than 80cm. When the length is greater than 80cm, the global behavior seems to be unchanged in cases of different concrete class. The resistance of RCS joint improves with the higher concrete class. The result for the initial stiffness shows that in all cases of the anchorage length, the joint initial stiffness is dependent on the concrete class. However the plastic bending moment is not much influenced by the different concrete class, especially for the anchorage length which is greater than 80cm.

**Conclusions**

In this article, a numerical study using ABAQUS software was conducted and its results were compared with the experimental tests for novel exterior RCS hybrid joint at the Structures Laboratory of INSA Rennes. After validating the suitable and reliable results, a set of parametric studies were conducted to investigate the influence of the anchorage length of the encased steel profile and the influence of the concrete class. Due to the previous results in this article, the following conclusions can be drawn:

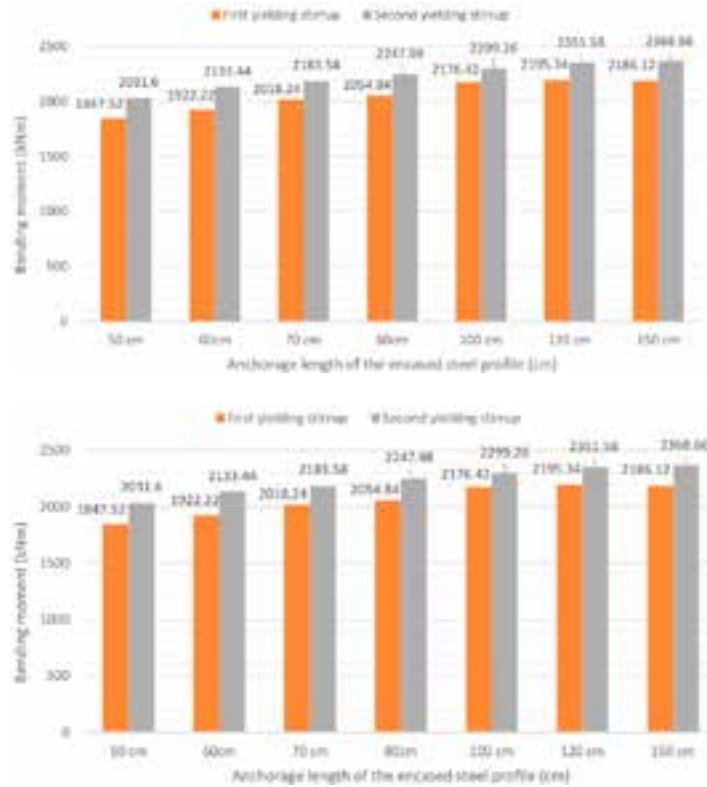


Figure 10. Bending moment corresponding to the yield stress in cases of different anchorage length

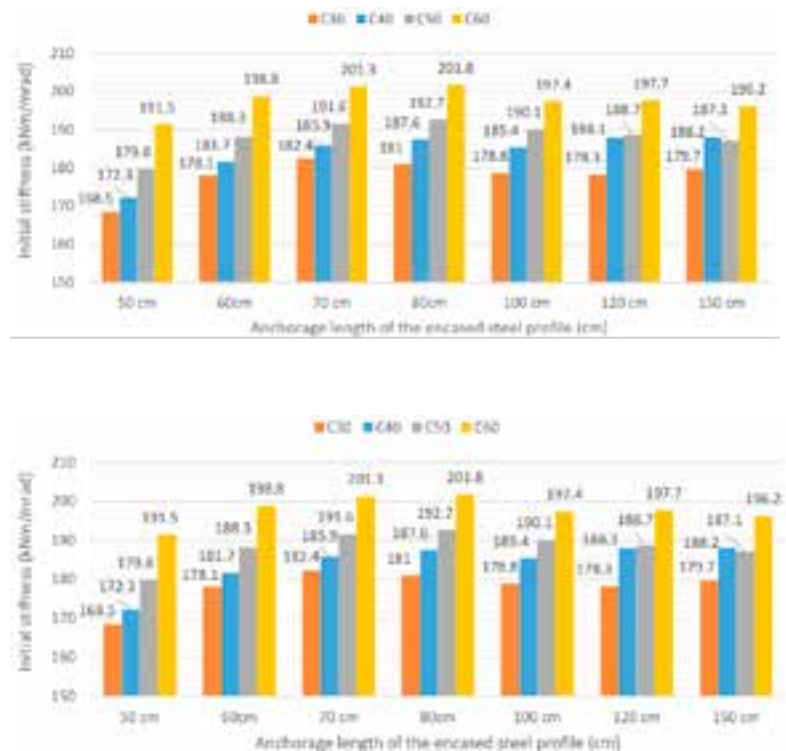


Figure 11. Plastic bending moment and initial stiffness in cases of different anchorage length

(xem tiếp trang 91)

for promoting economic, cultural and social growth. Furthermore, increasing road network has a great influence on the natural environment, society and the economy. The requirements for provinces and countries are to research and direct the development of road transport in a socioeconomically sustainable and effective manner. The article's study findings were based on a SWOT analysis to identify strengths and weaknesses, as well as challenges

and possibilities for developing the Dien Bien province's road transport system. After that, offer some solutions to overcome the flaws, enhance the strengths and possibilities for local road network development. It can be stated that the above solutions, if implemented properly, will contribute to the development of road network and create circumstances for the socioeconomic development of Dien Bien province./.

### References

1. Hung Nguyen (2020), *DienBien Transportation - Resources must be mobilized for synchronized growth*, on the website <https://tapchicongthuong.vn/>
2. *DienBien Province's Department of Transportation (2021), Report summarizing work in 2020 and tasks to be completed in 2021.*
3. Trinh Long (2021), *Dien Bien - Improve transportation infrastructure to create a driving force for development*, on the website <http://consosukien.vn/>
4. *DienBien Province People's Committee, Decision no.44/QĐ-UBND issued by the DienBien Province People's Committee on approving the adjustment of the Master Plan on the road network for the period 2011-2020, with a view toward 2030.*
5. Mohammed Alamgir and partners (2017), *Economic, Socio-Political and Environmental Risks of Road Development in the Tropics*, *Current Biology Review*.
6. Gede B. Suprayoga and partners (2017), *Coping with strategic ambiguity in planning sustainable road development: Balancing economic and environmental interests in two highway projects in Indonesia, Impact Assessment and Project Appraisal.*

## Study on a novel exterior RCS hybrid joint by ABAQUS

(tiếp theo trang 78)

- The numerical results were in good agreement with the experimental ones, both in terms of initial stiffness and ultimate loads.

- The numerical analysis by ABAQUS can be a reliable method to predict the exterior RCS hybrid joint behavior in monotonic loading.

- For anchorage length beyond 80cm, the joint stiffness, the plastic bending moment and the initial stiffness remain unchanged.

- The joint resistance improves with higher concrete class for anchorage length below 80cm. The latter remain unchanged for the anchorage length greater than 80cm. The plastic bending moment is not much affected by the difference of the concrete class while the joint initial stiffness dependent on the concrete class./.

### References

1. Zibasokhan, H., F. Behnamfar, and K. Behfarnia, *The new proposed details for moment resisting connections of steel beam to continuous concrete column. Advances in Structural Engineering*, 2016. 19(1): p. 156-169.
2. Nguyen, Q.-H., et al., *Finite Element analysis of a hybrid RCS beam-column connection.*, in *The 3rd International Conference CIGOS 2015 on « Innovations in Construction»*.2015: Paris, France, 11-12 May 2015.
3. Michal, S. and W. Andrzej, *Calibration of the cdp model parameters in abaqus. The 2015 World Congress on Advances in Structural Engineering and Mechanics (ASEM15), Incheon, Korea, 2015.*
4. Lubliner, J., et al., *A plastic-damage model for concrete. International Journal of Solids and Structures*, 1989: p. 299-326.
5. Lee, J. and G.L. Fenves, *A plastic-damage concrete model for earthquake analysis of dams. Earthquake Engineering & Structural Dynamics*, 1998. 27(9): p. 937-956.
6. Kmieciak, P. and M. Kaminski, *Modelling of reinforced concrete structures and composite structures with concrete strength degradation taken into consideration. Archives of Civil and Mechanical Engineering*, 2011. 11: p. 623-636.
7. Alfarah, B., F. Lopez-Almansa, and S. Oller, *New methodology for calculating damage variables evolution in plastic damage model for rc structures. 2017. 132: p. 70-86.*
8. *Eurocode-2, Design of concrete structures-Part 1: General rules and rules for buidings. EN1992-1-1. 2005: European Committee for Standardization.*
9. Kratzig, W.B. and R. Polling, *An elasto-plastic damage model for reinforced concrete with minimum number of material parameters. Computers & Structures*, 2004. 82(15-16): p. 1201-1215.